AAS 15-442

SOLAR SAIL EQUILIBRIA POINTS IN THE CIRCULAR RESTRICTED THREE BODY PROBLEM WITH ALBEDO EFFECTS

Mariusz E. Grøtte[*], **Marcus J. Holzinger**[†]

The Circular Restricted Three Body Problem (CR3BP) is investigated together with the effects of solar radiation pressure (SRP) and albedo radiation pressure acting on a solar sail spacecraft in a Sun-Asteroid system. Due to the significant albedo effects experienced close to an asteroid with highly reflective surfaces, the solar sail dynamics change considerably as compared to models investigated in previous work. For approximation purposes in establishing the albedo radiation, the asteroid is treated as a Lambertian diffuse model with characteristics from bi-directional reflectance distribution function (BRDF). As a result of both solar and albedo radiation, a wide range of artificial equilibrium solutions are generated in addition to the classical Lagrange points. Particular attention is given to the solutions around L_1 and L_2 with varying solar sail lightness numbers and orientation angles. The inclusion of albedo radiation effects indicates that the equilibrium points shift considerably as opposed to the model with SRP only, an important fact to address for any potential missions to bright objects such as asteroids and comets. Stability and controllability are investigated at the equilibrium points of interest, which are found to be unstable but controllable.

Keywords: Asteroids, Solar Sail, Circular Restricted Three Body Problem, Albedo Radiation, Lambertian Diffuse Models

INTRODUCTION

Space agencies worldwide have over the past decade executed several missions to primitive bodies such as asteroids and comets due to the rising interest from the scientific communities about understanding their environment, value as promising resource for mining and role as story-tellers about the creation of our Solar System.[1,2] In 2005 the Hayabusa mission, governed by Japan Aerospace Exploration Agency (JAXA), provided us more information about the dynamical environment of Asteroid 25143 Itokawa as well as samples from its surface.[3,4] In March 2015 the Dawn spacecraft is predicted to arrive at the dwarf planet Ceres for studying the relationship between the asteroid belt and formation of the Solar System.[5]

The option of solar sail propulsion has identified a wide range of mission applications. Main attributes of solar sails are more accessible long-term missions and controllable maneuvers at libration points naturally existing around primary masses in the Circular Restricted Three Body Prolem (CR3BP) through configurations such as Halo orbits these points.[6,7,8,9] Solar radiation pressure (SRP) and solar tide strength is claimed to alter the stability characteristics of the equilibrium points

[*]Graduate Student, Georgia Institute of Technology, Student AIAA Member
[†]Assistant Professor, Georgia Institute of Technology, Senior AIAA Member

when in the vicinity of the Sun, inducing the orbits to be easily controlled as discussed by J.A. Burns et al.[10] The paper emphasizes the importance of the solar radiation exerted on small particles. Furthermore, S.V. Ershkov provides analysis of a photogravitational restricted three body problem which can be linked to asteroids.[11] Studies have also been made about the dynamics of spacecraft orbits around comets, where it is claimed to be feasible that spacecraft may orbit the comet at Sun-side equilibrium points during its perihelion passage.[12]

Control methods applicable for spacecraft hovering over Near-Earth Asteroids (NEAs) are discussed by S.B. Broschart and D.J. Scheeres, which can ease the difficulty of orbiting small, irregularly sized and low-gravity objects.[13] The body-fixed hovering behavior maintains the spacecraft's relative position which can prove to be advantageous in acquiring high-resolution images of a particular surface. In fact, solar sails primarily utilize this hovering concept combined with surfing along equilibrium points induced by solar sail attitude or trimmed sail area. C.R. McInnes studies the available libration points for solar sails in CR3BP that are unstable in the Lyapunov sense, but establishes that they are controllable using feedback control to sail attitude alone.[8] In a simplified version of the solar sail, where it is modelled as a perfectly reflecting flat plate, these hovering points depend on sail attitude, acceleration and asteroid gravitational acceleration. Morrow et al. have investigated the solar sail CR3BP dynamics with the Hill approximation which applies well to the motion of spacecraft around asteroids.[14] The sail acceleration renders necessary restrictions when hovering and orbiting smaller bodies, due to inevitable sensitivities to perturbations. However, in general, it is claimed that the sailing capability offers potential low-cost missions and flexible methods for exploring the solar system.[15]

In order to establish analytical framework for study of SRP incorporated into the equations of motion (EoM), the initial steps are to investigate the CR3BP with SRP in a large mass-small mass system. This would be applicable for an asteroid heading towards the Sun or any other planet-asteroid system. In this paper, the formulation of the traditional three-body problem will be described together with derivation of the EoM including all significant assumptions. In this work, both gravitational and solar radiation force models for solar sail will be presented and defined in the Sun-Asteroid system. Main emphasis will be made on the dynamics of the solar sail in CR3BP with SRP, the effects of albedo exerted from the asteroid on the solar sail and how equilibrium solutions alter with varying solar sail lightness number and solar sail attitude angles.

The contributions in this paper are listed as follows: (a) modified contours of solar sail lightness number in a Sun-asteroid CR3BP system with albedo effects, modelled with Lambertian bi-directional reflectance distribution function (BRDF), are included; (b) extension to the solar sail CR3BP model with the existence of new on-axis and off-axis artificial equilibrium points are found with parametrized solar sail lightness number and solar sail orientation; (c) local stability analysis with albedo effects is established through linearized EoM, which shows that active control of the solar sail still is necessary at the unstable equilibrium points.

BACKGROUND

The dynamics of a solar sail in the CR3BP with SRP have previously established and serve as a model that is to be extended in this paper.[8,16] Both the large and small objects are treated as point masses moving around common center of mass denoted as m_1 and m_2, respectively. The detailed physics of SRP acting on a perfectly reflecting flat plate are discussed by McInnes.[16] The masses revolve around a common center of mass which defines the rotating reference frame $\mathcal{B}$: $\{\hat{\mathbf{x}}, \hat{\mathbf{y}}, \hat{\mathbf{z}}\}$ rotating with an angular velocity ${}^{\mathcal{I}}\boldsymbol{\omega}^{\mathcal{B}}$ with respect to the inertial frame $\mathcal{I}$: $\{\hat{\mathbf{i}}_1, \hat{\mathbf{i}}_2, \hat{\mathbf{i}}_3\}$. The di-

mensions are normalized so that the distance between the primary masses r_{12}, the sum of primary masses $m_1 + m_2$, angular velocity ${}^{\mathcal{I}}\boldsymbol{\omega}^{\mathcal{B}}$, and the gravitational constant G, are all defined to be unity. The mass ratio of the system is defined as $\mu = m_2/(m_1 + m_2)$. Figure 1 shows geometry of the CR3BP system.

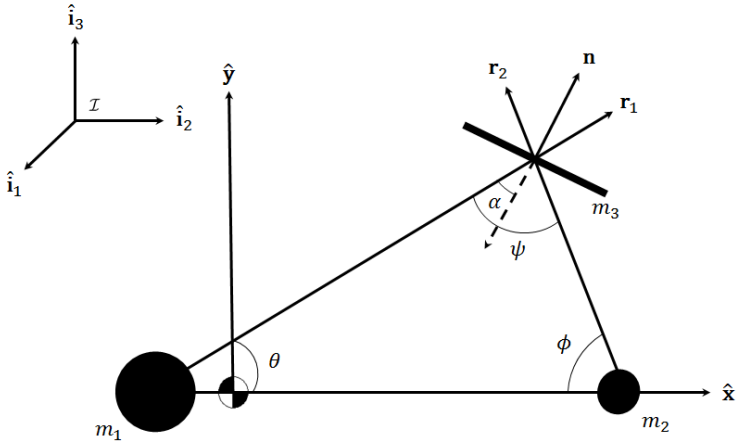

Figure 1. Schematic Geometry of the Solar Sail Restricted Three-Body Problem in the $\hat{\mathbf{x}} - \hat{\mathbf{y}}$ rotating frame.

The frame rotates once about the $\hat{\mathbf{z}}$-axis in time $2\pi/\omega$. By definition, the angular velocity ${}^{\mathcal{I}}\boldsymbol{\omega}^{\mathcal{B}}$ is equal to the mean motion and has a nondimensional magnitude equal to one. In this paper the dynamics are referred to the rotating $\mathcal{B}$ frame and notation for the frames will be dropped. Thus ${}^{\mathcal{I}}\boldsymbol{\omega}^{\mathcal{B}}$ can be expressed as,

$$\boldsymbol{\omega} = \hat{\mathbf{z}} \tag{1}$$

The position vectors for the solar sail with respect to m_1 and m_2 in the rotating frame, as seen in Figure 1, are defined as,

$$\mathbf{r_1} = [\,(x + \mu)\; y\; z\,]^{\,T} \tag{2}$$

$$\mathbf{r_2} = [\,(x - (1 - \mu))\; y\; z\,]^{\,T} \tag{3}$$

The solar sail is treated as massless and being only affected by gravity and radiative forces. The solar sail performance may be parametrized by the total spacecraft mass per unit area $\frac{m}{A}$ or sail loading σ. The sail pitch angle α may be expressed as the angle between the normal vector or sail attitude vector $\mathbf{n}$ and the incident radiation vector $\mathbf{r_1}$. Thus the acceleration due to radiation pressure can be expressed as,

$$\mathbf{a_1} = \beta \frac{G m_1}{r_1^2} \langle \hat{\mathbf{r}}_1 \cdot \mathbf{n} \rangle^2 \mathbf{n} \tag{4}$$

where m_1 is the mass of the large primary object (e.g. the Sun) and r_1 is the scalar distance from solar sail to m_1. Knowing that $\hat{\mathbf{r}}_\mathbf{1}$ is directed along the Sun-line and since the SRP force can never

be directed sunwards, the solar sail acceleration is constrained to be nonnegative.[8] Furthermore, with $\mathbf{n}$ being defined as the unit vector of the pseudo-potential $\boldsymbol{\nabla} U$, and since $\|\mathbf{n}\|_2 = 1$ then,

$$\mathbf{n} = \frac{\boldsymbol{\nabla} U}{\|\boldsymbol{\nabla} U\|_2} \tag{5}$$

$$\boldsymbol{\nabla} U = [U_x \; U_y \; U_z]^T \tag{6}$$

where

$$U_x = -\frac{(1-\mu)(x+\mu)}{r_1^3} - \frac{\mu(x-(1-\mu))}{r_2^3} \tag{7}$$

$$U_y = -\frac{(1-\mu)y}{r_1^3} - \frac{\mu y}{r_2^3} \tag{8}$$

$$U_z = -\frac{(1-\mu)z}{r_1^3} - \frac{\mu z}{r_2^3} \tag{9}$$

Therefore the $\langle \cdot \rangle$ term is the nonnegative operator and can be defined as,

$$\langle x \rangle = \begin{cases} x & \text{if } x \geq 0 \\ 0 & \text{if } x < 0 \end{cases}$$

The dimensionless sail loading parameter β is the defined as the ratio of the radiation pressure force to the solar gravitational force exerted on the sail, otherwise known as the lightness number of the solar sail.[8] This may be expressed as,

$$\beta = \frac{\sigma^*}{\sigma} \tag{10}$$

where

$$\sigma^* = \frac{\mathfrak{L}_1}{2\pi G m_1 c} \tag{11}$$

where $\mathfrak{L}_1$ is the luminosity of the large primary object, where for the Sun it is taken to be approximately $3.846 \times 10^{26}\ W$, and c is the speed of light. The vector form of EoM for a solar sail with $\mathbf{r}$ being the vector from the center of mass to m_3 can be defined in the rotating frame as,

$$\frac{d^2\mathbf{r}}{dt^2} + 2\boldsymbol{\omega} \times \frac{d\mathbf{r}}{dt} + \boldsymbol{\nabla} U = \mathbf{a_1} \tag{12}$$

Stationary solutions require the first two terms on the left hand side to vanish. With $\boldsymbol{\nabla} U = \mathbf{0}$ the five classical equilibrium points at $\mathbf{r_{L_i}} i = (1, ..., 5)$ can be found as the system is reduced to the conventional CR3BP. However, when including solar sail acceleration $\mathbf{a_1}$ then new artificial equilibrium solutions emerge.

The sail cone (pitch) angle, α and clock (precession) angle, γ, define the sail attitude with respect to the coordinate system $\mathcal{R}$: $\{\hat{\mathbf{r}}_\mathbf{1}, \hat{\mathbf{r}}_\mathbf{1} \times \hat{\mathbf{z}}, (\hat{\mathbf{r}}_\mathbf{1} \times \hat{\mathbf{z}}) \times \hat{\mathbf{r}}_\mathbf{1}\}$ centered on the solar sail. A schematic is shown in Figure 2. The angles may be written as,

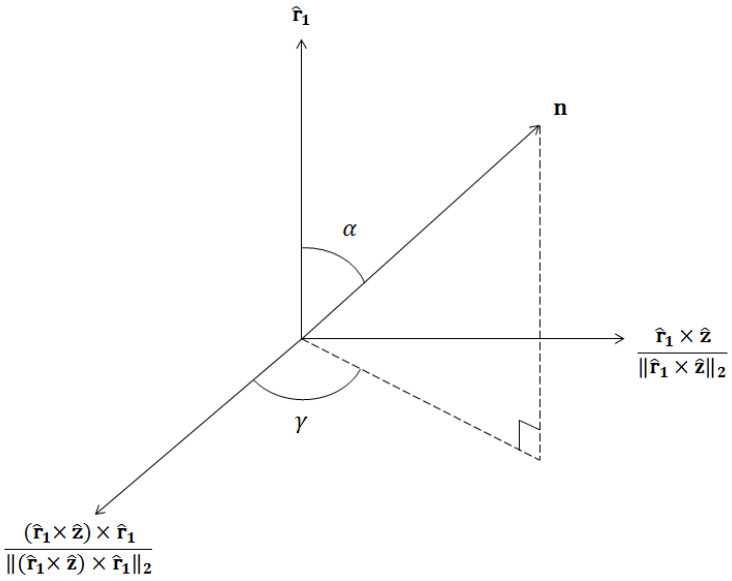

Figure 2. Definition of Solar Sail angles

$$\tan\alpha = \frac{\|\hat{\mathbf{r}}_1 \times \boldsymbol{\nabla} U\|_2}{\hat{\mathbf{r}}_1 \cdot \boldsymbol{\nabla} U} \tag{13}$$

$$\tan\gamma = \frac{\|((\hat{\mathbf{r}}_1 \times \hat{\mathbf{z}}) \times \hat{\mathbf{r}}_1) \times (\hat{\mathbf{r}}_1 \times \boldsymbol{\nabla} U)\|_2}{((\hat{\mathbf{r}}_1 \times \hat{\mathbf{z}}) \times \hat{\mathbf{r}}_1) \cdot (\hat{\mathbf{r}}_1 \times \boldsymbol{\nabla} U)} \tag{14}$$

The solar sail orientation can be expressed in terms of the components of $\mathbf{n}$ with respect to the rotating frame.[17] The scalar components of $\mathbf{n}$ corresponding to the directions $\hat{\mathbf{x}}$, $\hat{\mathbf{y}}$, $\hat{\mathbf{z}}$ are,

$$n_x = \frac{\cos\alpha(x+\mu)}{r_1} - \frac{\sin\alpha\cos\gamma(x+\mu)z}{\|(\mathbf{r}_1 \times \hat{\mathbf{z}}) \times \mathbf{r}_1\|_2} + \frac{\sin\alpha\sin\gamma y}{\|\mathbf{r}_1 \times \hat{\mathbf{z}}\|_2} \tag{15}$$

$$n_y = \frac{\cos\alpha y}{r_1} - \frac{\sin\alpha\cos\gamma yz}{\|(\mathbf{r}_1 \times \hat{\mathbf{z}}) \times \mathbf{r}_1\|_2} - \frac{\sin\alpha\sin\gamma(x+\mu)}{\|\mathbf{r}_1 \times \hat{\mathbf{z}}\|_2} \tag{16}$$

$$n_z = \frac{\cos\alpha z}{r_1} - \frac{\sin\alpha\cos\gamma(y^2 + (x+\mu)^2)}{\|(\mathbf{r}_1 \times \hat{\mathbf{z}}) \times \mathbf{r}_1\|_2} \tag{17}$$

With the solar sail orientation defined, then the effects of a solar sail may be added to the scalar EoM in the CR3BP. The solar sail acceleration may be expressed in scalar components with respect to rotating coordinates as,

$$a_x = \beta\frac{(1-\mu)}{r_1^2}\cos^2\alpha n_x \tag{18}$$

$$a_y = \beta\frac{(1-\mu)}{r_1^2}\cos^2\alpha n_y \tag{19}$$

$$a_z = \beta \frac{(1-\mu)}{r_1^2} \cos^2 \alpha n_z \tag{20}$$

Thus the compact form of EoM of the solar sail added with SRP are in the form,

$$\ddot{x} - 2\dot{y} = U_x + a_x \tag{21}$$

$$\ddot{y} + 2\dot{x} = U_y + a_y \tag{22}$$

$$\ddot{z} = U_z + a_z \tag{23}$$

Evaluating Eq. (12) and taking the scalar product of Eq. (6) with $\mathbf{n}$, and requiring equilibrium solutions, the solar lightness number may be expressed as,

$$\beta = \frac{r_1^2}{(1-\mu)} \frac{\boldsymbol{\nabla} U \cdot \mathbf{n}}{\langle \hat{\mathbf{r}}_\mathbf{1} \cdot \mathbf{n} \rangle^2} \tag{24}$$

The classical solutions without solar sail correspond to the subset $\beta = 0$. With $\beta > 0$ a particular equilibrium solution on a given surface is defined by the sail cone and clock attitude angles in Eq. (13) and Eq. (14).

In scalar form the three-body potential U may be written as,

$$U = -\left(\frac{1}{2}(x^2 + y^2) + \frac{1-\mu}{r_1} + \frac{\mu}{r_2} \right) \tag{25}$$

Evaluating the gradient of the potential U for the condition $\hat{\mathbf{r}}_\mathbf{1} \cdot \boldsymbol{\nabla} U = 0$, a function $S_1(\mathbf{r_1}) = 0$ is obtained as,

$$S_1(\mathbf{r_1}) = x(x+\mu) + y^2 - \frac{1-\mu}{r_1} - \mu \frac{\mathbf{r_1} \cdot \mathbf{r_2}}{r_2^3} \tag{26}$$

which defines regions where the solutions may exist and creates two topologically disconnected surfaces which define the boundary. Not only do the five classical Lagrange points lie on these surfaces since they are solutions to $\boldsymbol{\nabla} U = \mathbf{0}$ but, in general, the sail loading surfaces also approach the boundary asymptotically with $\beta \to \infty$ since $\hat{\mathbf{r}}_\mathbf{1} \cdot \boldsymbol{\nabla} U \to 0$. It can easily be seen that $S_1(\mathbf{r_1})$ does not explicitly depend on SRP and that $S_1(\mathbf{r_1}) < 0$ gives regions of x,y,z for which the EoM are valid and that the solar sail is in tension.

THEORY

Based on the EoM in CR3BP with SRP effects presented, the model is now extended to include the albedo effects exerted on the solar sail when close to a primitive body m_2 such as an asteroid. As an approximation, luminosity of the asteroid is firstly characterized by the BRDF and secondly it is treated as an Lambertian diffuse model. It is known that for Lambertian BRDF, the reflecting radiation can be expressed as a function of the angle between the sun-line vector $\hat{\mathbf{r}}_\mathbf{12}$ with respect to the body m_2 and the viewer line of sight $\hat{\mathbf{r}}_\mathbf{2}$. Therefore with the asteroid's albedo radiation exerted on the solar sail, the Lambertian BRDF may be expressed as in terms of a function of $\rho p(\phi)$ where ρ is albedo reflectance and $p(\phi)$ is the diffuse phase angle function.[18] $p(\phi)$ may be defined as,

$$p(\phi) = \frac{2}{3\pi}(\sin\phi + (\pi - \phi)\cos\phi) \tag{27}$$

Several techniques have been developed to estimate albedo values.[19,20] It has been common to establish that a reasonable reflectance value for asteroids should be $\rho = 0.1 - 0.2$[21,22] and that they are treated as gray bodies, such that ρ is constant for all wavelengths, which is consistent with previous studies.[18] Furthemore the technique of optical signatures have frequently used the visual magnitude system, adopted from the astronomers. This method will also be applied here and serves as an approximation tool.

The optical signature magnitude of an asteroid M_2, when approximated as a sphere, is given by

$$M_2 = M_1 - 2.5\log\left(\frac{d_2^2}{r_2^2}\rho p(\phi)\right) \tag{28}$$

where d_2 is the diameter of the asteroid and r_2 is the distance between the asteroid and the observing spacecraft. M_1 (optical signature magnitude of the Sun) has the visual magnitude of -26.73 from the Earth.[18] For a fixed diameter d_2 and albedo ρ of the smaller primary m_2, a function of ϕ and r_2 is obtained from rearranging Eq. 28 and is of the form

$$F(\phi, r_2, \rho; d_2) = \frac{d_2^2}{r_2^2}\rho p(\phi) \tag{29}$$

In this paper the function $F(\phi, r_2, \rho; d_2)$ will from now and onwards be written as F. The apparent luminosity of the asteroid can be defined in terms of the luminosity of the Sun m_1 as

$$\mathfrak{L}_2 = \mathfrak{L}_1 F \tag{30}$$

Therefore the acceleration of the solar sail due albedo effects from the asteroid may be expressed as

$$\mathbf{a_2} = \tilde{\beta}\frac{Gm_2}{r_2^2}\langle\hat{\mathbf{r}}_\mathbf{2}\cdot\mathbf{n}\rangle^2\mathbf{n} \tag{31}$$

where

$$\tilde{\beta} = \frac{\mathfrak{L}_2}{2\pi G m_2 c\sigma} \tag{32}$$

The relationship between β and $\tilde{\beta}$ is of the form

$$\begin{aligned}\frac{\tilde{\beta}}{\beta} &= \frac{m_1}{m_2}\frac{\mathfrak{L}_2}{\mathfrak{L}_1} \\ &= \frac{(1-\mu)}{\mu}F\end{aligned} \tag{33}$$

$$\Rightarrow \tilde{\beta} = \beta\frac{(1-\mu)}{\mu}F \tag{34}$$

With the sail cone angle α and clock angle γ defined, the sail attitude with respect to $\mathbf{r_2}$ can be defined as $(\psi - \alpha)$, and from using trigonometric identities then,

$$\begin{aligned}\tan(\psi - \alpha) =& \frac{\|\hat{\mathbf{r}}_\mathbf{2} \times \boldsymbol{\nabla} U\|_2}{\hat{\mathbf{r}}_\mathbf{2} \cdot \boldsymbol{\nabla} U} \\ =& \frac{(\|\hat{\mathbf{r}}_\mathbf{1} \times \hat{\mathbf{r}}_\mathbf{2}\|_2)(\hat{\mathbf{r}}_\mathbf{1} \cdot \boldsymbol{\nabla} U) - (\hat{\mathbf{r}}_\mathbf{1} \cdot \hat{\mathbf{r}}_\mathbf{2})(\|\hat{\mathbf{r}}_\mathbf{1} \times \boldsymbol{\nabla} U\|_2)}{(\hat{\mathbf{r}}_\mathbf{1} \cdot \hat{\mathbf{r}}_\mathbf{2})(\hat{\mathbf{r}}_\mathbf{1} \cdot \boldsymbol{\nabla} U) + (\|\hat{\mathbf{r}}_\mathbf{1} \times \hat{\mathbf{r}}_\mathbf{2}\|_2)(\|\hat{\mathbf{r}}_\mathbf{1} \times \boldsymbol{\nabla} U\|_2)}\end{aligned} \tag{35}$$

Evaluating Eq. (12) with $\mathbf{a_2}$ instead of $\mathbf{a_1}$ and taking the scalar product of Eq. (6) with $\mathbf{n}$, and requiring equilibrium solutions, the solar lightness number may be expressed as

$$\beta = \frac{\boldsymbol{\nabla} U \cdot \mathbf{n}}{(1-\mu)\left(\frac{1}{r_1^2}\langle \hat{\mathbf{r}}_\mathbf{1} \cdot \mathbf{n}\rangle^2 + F\frac{1}{r_2^2}\langle \hat{\mathbf{r}}_\mathbf{2} \cdot \mathbf{n}\rangle^2\right)} \tag{36}$$

It is easy to see that with $\rho = 0$ or $F = 0$, the problem is identical to the solar sail CR3BP with SRP.

Evaluating the gradient of the pseudo-potential U for the condition $\hat{\mathbf{r}}_\mathbf{2} \cdot \boldsymbol{\nabla} U \geq 0$, a function $S_2(\mathbf{r_1}) = 0$ is obtained

$$S_2(\mathbf{r_1}) = x(x + \mu - 1) + y^2 - (1-\mu)\frac{\mathbf{r_2} \cdot \mathbf{r_1}}{r_1^3} - \frac{\mu}{r_2} \tag{37}$$

which defines the boundary, affected by albedo radiation pressure. The surfaces are in this case also disconnected which define the boundary to the regions of where equilibrium solutions exist. Both radiation pressure accelerations $\mathbf{a_1}$ and $\mathbf{a_2}$ cause the solar sail to operate in tension. The equilibrium solutions must exist in the intersection of the two functions $S_1(\mathbf{r_1}) = 0$ and $S_2(\mathbf{r_1}) = 0$ which is an extension to the two boundaries defined in Eq.26 and Eq.37. As usual with $\boldsymbol{\nabla} U = \mathbf{0}$, the five classical equilibrium points can be found as the equations are reduced to the classical CR3BP.

Now that the solar sail dynamics in CR3BP with SRP have been properly defined, it is worth looking into the stability of these equilibrium solutions and how to control the spacecraft at these fixed points. However, time-variant dynamics and control of solar sail along periodic trajectories are not investigated in this paper and are left for future work.

Stability and Control at Libration Points

In reality, the motion of a spacecraft in CR3BP is highly nonlinear and complex. In order to investigate stability and controllability, the behavior of the system is analyzed using local linear dynamics about the chosen equilibrium points of interest (e.g. the Lagrangian points or artificial equilibrium points).[8]

The equilibrium (libration) points have the coordinates $(x_{L_i}, y_{L_i}, z_{L_i})$ which are in the rotating reference frame and L_i is the equilibrium point of interest. With perturbation the coordinates (ξ, η, ζ) can be written as,

$$\mathbf{r_{L_i}} + \delta\mathbf{r} = [(x_{Li} + \xi)\ \ (y_{Li} + \eta)\ \ (z_{Li} + \zeta)]^T \tag{38}$$

With only first order terms considered, then the local solar sail EoM with respect to the equilibrium points at $\mathbf{r_{L_i}}$ (denoted with '*') can be expressed as,

$$\ddot{\xi} - 2\dot{\eta} = (U^*_{xx} + a^*_{1,xx})\xi + (U^*_{xy} + a^*_{1,xy})\eta + (U^*_{xz} + a^*_{1,xz})\zeta \tag{39}$$

$$\ddot{\eta} + 2\dot{\xi} = (U^*_{yx} + a^*_{1,yx})\xi + (U^*_{yy} + a^*_{1,yy})\eta + (U^*_{yz} + a^*_{1,yz})\zeta \tag{40}$$

$$\ddot{\zeta} = (U^*_{zx} + a^*_{1,zx})\xi + (U^*_{zy} + a^*_{1,zy})\eta + (U^*_{zz} + a^*_{1,zz})\zeta \tag{41}$$

where $U_{jk} = \frac{\partial U}{\partial j \partial k}$ and $U^*_{jk} = U_{jk}|_{L_i}$ where $(j,k) \in (x,y,z)$. The second partials of the acceleration is defined as $a_{1,jk} = \frac{\partial a_1}{\partial j \partial k}$ and is the kth derivative of the jth component, and furthermore $a^*_{1,jk} = a_{1,jk}|_{L_i}$.

In state space form this can be written as,

$$\dot{\tilde{\mathbf{x}}} = \mathbf{A}\tilde{\mathbf{x}} \tag{42}$$

where the state vector is defined as $\tilde{\mathbf{x}} = [\, \xi \; \eta \; \zeta \; \dot{\xi} \; \dot{\eta} \; \dot{\zeta}\,]^{\,T}$ and the state matrix is defined as

$$\mathbf{A} = \begin{bmatrix} \mathbf{0}_{3\times 3} & \mathbb{I}_{3\times 3} \\ \mathbf{T} & \mathbf{N} \end{bmatrix} \tag{43}$$

where

$$\mathbf{T} = \begin{bmatrix} U_{xx} + a_{1,xx} & U_{xy} + a_{1,xy} & U_{xz} + a_{1,xz} \\ U_{yx} + a_{1,yx} & U_{yy} + a_{1,yy} & U_{yz} + a_{1,yz} \\ U_{zx} + a_{1,zx} & U_{zy} + a_{1,zy} & U_{zz} + a_{1,zz} \end{bmatrix} \tag{44}$$

$$\mathbf{N} = \begin{bmatrix} 0 & 2 & 0 \\ -2 & 0 & 0 \\ 0 & 0 & 0 \end{bmatrix} \tag{45}$$

For a nontrivial solution, then taking $\det(\mathbf{A}) = 0$ gives the characteristic polynomial[8]

$$\mathfrak{P}(\lambda) = \sum_{j=0}^{6} q_j \lambda^{6-j} \tag{46}$$

From evaluating the characteristic polynomial, the solutions to the local linear dynamics about the equilibrium point L_i will have the following form,[17]

$$\xi(t) = \sum_{i=1}^{6} k_i e^{\lambda_i t} \tag{47}$$

$$\eta(t) = \sum_{i=1}^{6} l_i e^{\lambda_i t} \tag{48}$$

$$\zeta(t) = \sum_{i=1}^{6} m_i e^{\lambda_i t} \tag{49}$$

where $\lambda_{i=1,\ldots,6}$ represent the eigenvalues of the $\mathbf{A}$ matrix. If the selected point is an equilibrium point defined in the $\hat{\mathbf{x}} - \hat{\mathbf{y}}$ plane then,

$$U^*_{xz} + a^*_{1,xz} = U^*_{yz} + a^*_{1,yz} = U^*_{zx} + a^*_{1,zx} = U^*_{zy} + a^*_{1,zy} = 0 \tag{50}$$

Likewise for $\hat{\mathbf{x}} - \hat{\mathbf{z}}$ plane then,

$$U^*_{xy} + a^*_{1,xy} = U^*_{yz} + a^*_{1,yz} = U^*_{yx} + a^*_{1,yx} = U^*_{zy} + a^*_{1,zy} = 0 \tag{51}$$

This results in decoupling of the out-of-plane equations associated with ζ, thus the relationship between k_i and l_i in the $\hat{\mathbf{x}} - \hat{\mathbf{y}}$ plane can be written as,

$$l_i = \frac{\lambda_i^2 - (U^*_{xx} + a^*_{1,xx})}{2\lambda_i + (U^*_{xy} + a^*_{1,xy})} k_i \tag{52}$$

Based on Lyapunov Stability Theory then the following statements are true,[23]

i) $\mathbf{A}$ is *Lyapunov stable* if spec($\mathbf{A}$) $\subset$ CLHP and, if $\lambda_{i=1,\ldots,6} \in$ spec($\mathbf{A}$) and Re $(\lambda_i) = 0$, then λ_i is semisimple (algebraic multiplicity = geometric multiplicity).

ii) $\mathbf{A}$ is *semistable* if spec($\mathbf{A}$) $\subset$ OLHP $\cup \{0\}$ and, if $0 \in$ spec($\mathbf{A}$) then 0 is semisimple.

iii) $\mathbf{A}$ is *asymptotically stable* if spec($\mathbf{A}$) $\subset$ OLHP.

iv) $\mathbf{A}$ is *unstable* if $\mathbf{A}$ is not Lyapunov stable.

where spec$(\mathbf{A})$ is the spectrum of $\mathbf{A}$ containing the its eigenvalues $\lambda_{i=1,\ldots,6}$, CLHP is the closed left half complex plane i.e. Re$(\lambda_i) \leq 0$, OLHP is the open left half complex plane i.e. Re$(\lambda_i) < 0$.

It is known that in the system without SRP the collinear libration points, L_1, L_2, L_3, are unstable and the initial conditions can at best be chosen such that the eigenvalues are not excited, meaning Lyapunov stability near the collinear points.[24]

The coefficients of the polynomial $\mathfrak{P}(\lambda)$ are given by,[8]

$$q_6 = \mathbf{T}^*_{11}(\mathbf{T}^*_{22}\mathbf{T}^*_{33} - \mathbf{T}^*_{23}\mathbf{T}^*_{32}) - \mathbf{T}^*_{12}(\mathbf{T}^*_{33}\mathbf{T}^*_{21} - \mathbf{T}^*_{23}\mathbf{T}^*_{31}) - \mathbf{T}^*_{13}(\mathbf{T}^*_{22}\mathbf{T}^*_{31} - \mathbf{T}^*_{21}\mathbf{T}^*_{32}) \tag{53a}$$
$$q_5 = 2\mathbf{T}^*_{33}(\mathbf{T}^*_{21}\mathbf{T}^*_{12}) + 2(\mathbf{T}^*_{32}\mathbf{T}^*_{13} - \mathbf{T}^*_{23}\mathbf{T}^*_{31}) \tag{53b}$$
$$q_4 = \mathbf{T}^*_{11}\mathbf{T}^*_{22} + \mathbf{T}^*_{11}\mathbf{T}^*_{33} + \mathbf{T}^*_{23}\mathbf{T}^*_{32} - \mathbf{T}^*_{13}\mathbf{T}^*_{31} - \mathbf{T}^*_{12}\mathbf{T}^*_{21} + 4\mathbf{T}^*_{33} \tag{53c}$$
$$q_3 = 2(\mathbf{T}^*_{21} - \mathbf{T}^*_{12}) \tag{53d}$$
$$q_2 = \mathbf{T}^*_{11} + \mathbf{T}^*_{22} + \mathbf{T}^*_{33} + 4 \tag{53e}$$
$$q_1 = 0 \tag{53f}$$
$$q_0 = 1 \tag{53g}$$

To check if the system is stable then according to the Routh-Hurwitz criterion, then for a nth-degree polynomial $\mathfrak{P}(\lambda)$, all coefficients q_i must exist ($q_i \neq 0$), be positive $q_i > 0$ and if there is any sign change in the Routh Array then it means that the system is unstable. Looking at the Eq.53a-53g implies that at least one eigenvalue will not lie in CLHP since $q_1 = 0$. Thus the system is naturally unstable. Substituting for purely imaginary eigenvalues $\lambda = \iota\kappa$ ($\iota = \sqrt{-1}$), the characteristic polynomial becomes,[8]

$$\mathfrak{P}(\iota\kappa) = -\kappa^6 + q_2\kappa^4 - \iota q_3\kappa^3 - q_4\kappa^2 + \iota q_5\kappa + q_6 \tag{54}$$

For the condition $\mathfrak{P}(\lambda) = 0$ then both real and purely imaginary parts are identically zero, thus,

$$\kappa^6 + q_2\kappa^4 - q_4\kappa^2 + q_6 = 0 \tag{55a}$$

$$\iota\kappa(q_5 - \kappa^2 q_3) = 0 \tag{55b}$$

Six solutions appear from this set of equations with $\kappa_i^2 > 0$, $i = (1, ..., 6)$. With $\kappa_1 = 0$ and $\kappa_{2,3} = \pm\sqrt{\frac{q_5}{q_3}}$, the solution κ is not a consistent solution. The latter equation can be satisfied if $q_3 = q_5 = 0$ and are then represented as conjugate pairs in the first equation which may or may not have real solutions. In order to have Lyapunov stability then, by necessity, $q_3 = 0 \Rightarrow (\mathbf{B}_{21}^* - \mathbf{B}_{12}^*) = 0$. Since potential is conservative $U_{yx} - U_{xy} = 0$, such that $q_3 = 0 \Rightarrow (a_{1,yx} - a_{1,xy}) = 0$. With $q_5 = 0$ it is also required that $(a_{1,zx} - a_{1,xz}) = 0$ and $(a_{1,yz} - a_{1,zy}) = 0$. This implies that $\beta = 0$ or

$$\boldsymbol{\nabla} \times \mathbf{a_1} = \mathbf{0} \tag{56}$$

Only for conservative systems is the curl of a vector zero. This implies that solar radiation pressure must be conservative and must be derived from some scalar potential.[8] A requirement for Lyapunov stability is therefore that solar radiation pressure force is zero, i.e. $\beta = 0$, or the problem is conservative, i.e. $\alpha = 0^\circ$. Although the equilibrium solutions are in general unstable, they are controllable using either feedback to the sail attitude or trims to the sail area. Enforcing local linear stability, i.e. all Re(λ_i) < 0, can be done by pole placement method or optimal control.

In this paper the sail position and velocity controllability will be investigated using the solar sail attitude as the control input, which is considered to be more practical than trimming area of the solar sail by varying β as there is more flexibility in changing the attitude by two control variables only. Nevertheless, in future work, it is worth to examine controllability with three control variables as the thrust of the solar sail has three components.[17] The sail orientation control variables are defined such that the input is,

$$\mathbf{u}^* + \delta\mathbf{u} = [\alpha_{L_i} + \delta\alpha \;\; \gamma_{L_i} + \delta\gamma]^T \tag{57}$$

where α_{L_i} and γ_{L_i} are the nominal sail angles corresponding to the libration point of interest. Thus the state space form becomes,

$$\dot{\tilde{\mathbf{x}}} = \mathbf{A}\tilde{\mathbf{x}} + \mathbf{B}\delta\mathbf{u} \tag{58}$$

where $\mathbf{A}$ is the same as before and $\mathbf{B}$ has the form,

$$\mathbf{B} = \begin{bmatrix} 0 & 0 \\ 0 & 0 \\ 0 & 0 \\ a^*_{1,x\alpha} & a^*_{1,x\gamma} \\ a^*_{1,y\alpha} & a^*_{1,y\gamma} \\ a^*_{1,z\alpha} & a^*_{1,z\gamma} \end{bmatrix} \tag{59}$$

The controllability matrix $\mathbf{\Gamma} \in \mathbb{R}^{6\times 12}$ can be written as,

$$\mathbf{\Gamma} = \begin{bmatrix} \mathbf{B} & \mathbf{AB} & \mathbf{A}^2\mathbf{B} & \mathbf{A}^3\mathbf{B} & \mathbf{A}^4\mathbf{B} & \mathbf{A}^5\mathbf{B} \end{bmatrix} \tag{60}$$

For the system to be completely controllable, then for $\mathbf{A} \in \mathbb{R}^{6\times 6}$ and $\mathbf{B} \in \mathbb{R}^{6\times 2}$ the following is a necessary and sufficient condition,

$$\text{rank}(\mathbf{\Gamma}) = 6 \tag{61}$$

It is found that $\mathbf{\Gamma}$ has full rank if the solar sail is not oriented parallell to the SRP force (when $\alpha = \pm 90°$).[8] Since,

$$\mathbf{B} \neq \mathbf{0}_{6\times 2} \tag{62}$$

if $\hat{\mathbf{r}}_\mathbf{1} \cdot \mathbf{n} \neq 0$, then this implies that the columns of $\mathbf{\Gamma}$ are linearly independent, thus rank$(\mathbf{\Gamma}) = 6$ and the system is completely controllable. If $\hat{\mathbf{r}}_\mathbf{1} \cdot \mathbf{n} = 0$ or equivalently $\alpha = \pm 90°$, then the input has no influence on the state dynamics and the system is uncontrollable.

Stability and Control at Libration Points with Albedo Radiation

With the asteroid reflecting radiative forces, then now the perturbations will be induced by additional effects from the albedo radiation exerted on the solar sail. Thus the state matrix $\mathbf{A}$ will change and referring to Eq. 44, the T matrix will have the form,

$$\mathbf{T} = \begin{bmatrix} U_{xx} + a_{1,xx} + a_{2,xx} & U_{xy} + a_{1,xy} + a_{2,xy} & U_{xz} + a_{1,xz} + a_{2,xz} \\ U_{yx} + a_{1,yx} + a_{2,yx} & U_{yy} + a_{1,yy} + a_{2,yy} & U_{yz} + a_{1,yz} + a_{2,yz} \\ U_{zx} + a_{1,zx} + a_{2,zx} & U_{zy} + a_{1,zy} + a_{2,zy} & U_{zz} + a_{1,zz} + a_{2,zz} \end{bmatrix} \tag{63}$$

With only first order terms considered, then the perturbation EoM with respect to the equilibrium point can now be expressed as,

$$\ddot{\xi} - 2\dot{\eta} = (U^*_{xx} + a^*_{1,xx}a^*_{2,xx})\xi + (U^*_{xy} + a^*_{1,xy} + a^*_{2,xy})\eta + (U^*_{xz} + a^*_{1,xz} + a^*_{2,xz})\zeta \tag{64}$$

$$\ddot{\eta} + 2\dot{\xi} = (U^*_{yx} + a^*_{1,yx} + a^*_{2,yx})\xi + (U^*_{yy} + a^*_{1,yy} + a^*_{2,yy})\eta + (U^*_{yz} + a^*_{1,yz} + a^*_{2,yz})\zeta \tag{65}$$

$$\ddot{\zeta} = (U^*_{zx} + a^*_{1,zx} + a^*_{2,zx})\xi + (U^*_{zy} + a^*_{1,zy} + a^*_{2,zy})\eta + (U^*_{zz} + a^*_{1,zz} + a^*_{2,zz})\zeta \tag{66}$$

where $a_{j,kl} = \frac{\partial a_j}{\partial k \partial l}$ and is the lth derivative of the kth component of the radiation acceleration vector $\mathbf{a_j}$ with respect to body m_j $j \in (1,2)$, and furthermore $a^*_{j,kl} = a_{j,kl}|_{L_i}$.

By applying the Routh-Hurwitz criterion in the same manner as previously, it is found that the coefficients of the polynomial $\mathfrak{P}(\lambda)$ are given by,

$$q_6 = \mathbf{T}^*_{11}(\mathbf{T}^*_{22}\mathbf{T}^*_{33} - \mathbf{T}^*_{23}\mathbf{T}^*_{32}) - \mathbf{T}^*_{12}(\mathbf{T}^*_{33}\mathbf{T}^*_{21} - \mathbf{T}^*_{23}\mathbf{T}^*_{31}) - \mathbf{T}^*_{13}(\mathbf{T}^*_{22}\mathbf{T}^*_{31} - \mathbf{T}^*_{21}\mathbf{T}^*_{32}) \tag{67a}$$

$$q_5 = 2\mathbf{T}^*_{33}(\mathbf{T}^*_{21}\mathbf{T}^*_{12}) + 2(\mathbf{T}^*_{32}\mathbf{T}^*_{13} - \mathbf{T}^*_{23}\mathbf{T}^*_{31}) \tag{67b}$$

$$q_4 = \mathbf{T}^*_{11}\mathbf{T}^*_{22} + \mathbf{T}^*_{11}\mathbf{T}^*_{33} + \mathbf{T}^*_{23}\mathbf{T}^*_{32} - \mathbf{T}^*_{13}\mathbf{T}^*_{31} - \mathbf{T}^*_{12}\mathbf{T}^*_{21} + 4\mathbf{T}^*_{33} \tag{67c}$$

$$q_3 = 2(\mathbf{T}^*_{21} - \mathbf{T}^*_{12}) \tag{67d}$$

$$q_2 = \mathbf{T}^*_{11} + \mathbf{T}^*_{22} + \mathbf{T}^*_{33} + 4 \tag{67e}$$

$$q_1 = 0 \tag{67f}$$

$$q_0 = 1 \tag{67g}$$

Looking at the Eq. 67a-67g implies that at least one eigenvalue will not lie in CLHP since $q_1 = 0$. Thus the system is naturally unstable. Substituting for purely imaginary eigenvalues, the characteristic polynomial becomes,

$$\mathfrak{P}(\iota\kappa) = -\kappa^6 + q_2\kappa^4 - \iota q_3\kappa^3 - q_4\kappa^2 + \iota q_5\kappa + q_6 \tag{68}$$

For the condition $\mathfrak{P}(\lambda) = 0$ then both real and purely imaginary parts are identically zero, thus,

$$\kappa^6 + q_2\kappa^4 - q_4\kappa^2 + q_6 = 0 \tag{69a}$$

$$\iota\kappa(q_5 - \kappa^2 q_3) = 0 \tag{69b}$$

Six solutions appear from this set of equations with $\kappa_i^2 > 0$, $i = (1, ..., 6)$. With $\kappa_1 = 0$ and $\kappa_{2,3} = \pm\sqrt{\frac{q_5}{q_3}}$, the solution κ is not a consistent solution. The latter equation can be satisfied if $q_3 = q_5 = 0$ and are then represented as conjugate pairs in the first equation which may or may not have real solutions. In order to have Lyapunov stability then, by necessity, $q_3 = 0 \Rightarrow (\mathbf{B}^*_{21} - \mathbf{B}^*_{12}) = 0$. Since potential is conservative $U_{yx} - U_{xy} = 0$, such that $q_3 = 0 \Rightarrow (a_{1,yx} + a_{2,yx} - a_{1,xy} - a_{2,xy}) = 0$. With $q_5 = 0$ it is also required that $(a_{1,zx} + a_{2,zx} - a_{1,xz} - a_{2,xz}) = 0$ and $(a_{1,yz} + a_{2,yz} - a_{1,zy} - a_{2,zy}) = 0$. This implies that $\beta = 0$ or,

$$\boldsymbol{\nabla} \times \mathbf{a_1} + \boldsymbol{\nabla} \times \mathbf{a_2} = \mathbf{0} \tag{70}$$

$$\Rightarrow \boldsymbol{\nabla} \times \mathbf{a_1} = -\boldsymbol{\nabla} \times \mathbf{a_2} \tag{71}$$

Similar to the CR3BP with SRP acceleration $\mathbf{a_1}$ only, this implies that the solar radiation pressure from both $\mathbf{a_1}$ and $\mathbf{a_2}$ must be either conservative or one of the accelerations must be balanced by opposite curl. A requirement for Lyapunov stability is therefore that solar radiation pressure force is zero, i.e. $\beta = 0$, or the problem is conservative, i.e. $\alpha = 0^\circ$ and $\psi = 90^\circ$, or the

radiation pressure accelerations are balanced, i.e. $\mathbf{a_1} = -\mathbf{a_2}$. The modified stability characteristics are part of contribution (c). Although the equilibrium solutions are in general still unstable, they are controllable using either feedback to the sail attitude or trims to the sail area. Enforcing local linear stability, i.e. all eigenvalues to be $\text{Re}(\lambda_i) < 0$, can be done by pole placement method or optimal control.

With the same control variables as defined in Eq. 57 and referring to Eq. 59, the $\mathbf{B}$ matrix will now have the form:

$$\mathbf{B} = \begin{bmatrix} 0 & 0 \\ 0 & 0 \\ 0 & 0 \\ a^*_{1,x\alpha} + a^*_{2,x\alpha} & a^*_{1,x\gamma} + a^*_{2,x\gamma} \\ a^*_{1,y\alpha} + a^*_{2,y\alpha} & a^*_{1,y\gamma} + a^*_{2,y\gamma} \\ a^*_{1,z\alpha} + a^*_{2,z\alpha} & a^*_{1,z\gamma} + a^*_{2,z\gamma} \end{bmatrix} \tag{72}$$

where $a_{j,kl} = \frac{\partial a_j}{\partial k \partial l}$ and is the lth derivative of the kth component of the radiation acceleration vector $\mathbf{a_j}$ with respect to body m_j, $j \in (1, 2)$, and furthermore $a^*_{j,kl} = a_{j,kl}|_{L_i}$.

It is found that the modified controllability matrix $\mathbf{\Gamma}$ has full rank except when the solar sail is not oriented parallell to the radiation forces from m_1 and m_2 having the properties $\hat{\mathbf{r}}_\mathbf{1} \cdot \mathbf{n} = 0$ and $\hat{\mathbf{r}}_\mathbf{2} \cdot \mathbf{n} = 0$ (when $\alpha = \pm 90^\circ$ and $\psi = 0^\circ$), which is naturally similar to the CR3BP with SRP acceleration $\mathbf{a_1}$ alone when the system is uncontrollable if $\hat{\mathbf{r}}_\mathbf{1} \cdot \mathbf{n} = 0$. This is another part of the contribution (c) in this paper. This implies that the columns of $\mathbf{\Gamma}$ are linearly independent if $\hat{\mathbf{r}}_\mathbf{1} \cdot \mathbf{n} \neq 0$ and $\hat{\mathbf{r}}_\mathbf{2} \cdot \mathbf{n} \neq 0$ simultaneously, thus $\text{rank}(\mathbf{\Gamma}) = 6$ and the system is completely controllable.

If the system is completely controllable, then a feedback gain $\mathbf{K}$ may be constructed from pole placement by arbitrarily placing eigenvalues such that $\text{Re}(\lambda_i) < 0$ or optimal control such that the closed-loop system $\mathbf{A_{cl}} = (\mathbf{A} + \mathbf{BK})$ is asymptotically stable.

NUMERICAL RESULTS

Analyzing the planar CR3BP for two separate cases: $y = 0$ and $z = 0$ the solar sail in the Sun-Asteroid system with varying β and orientations (α, γ), it is clear that the classical libration points $L_{1,\ldots,5}$ are replaced by infinitely many artificial equilibrium points when including radiation pressure from both the Sun and the asteroid.

For the results discussed here, the mass ratio is chosen to be $\mu \approx 1.302543991786095 \times 10^{-10}$, $\rho = 0.2$, $d_2 = 525.4\, km$ and $r_{12} = 353.268 \times 10^6\, km$ which are geometrical and physical parameters equivalent to an asteroid representing Vesta, which is a large asteroid residing in the asteroid field. Previous studies have been made on how SRP generates artificial equilibrium points, however, with albedo radiation these equilibrium points change considerably and solar lightness number contours become altered due to Lambertian BRDF reflectance as a function of ϕ and r_2. The chosen region to investigate is in the vicinity of L_1 and L_2.

Figure 3 and 4 shows some of the equilibrium solutions or contours of solar sail lightness number β in the CR3BP with SRP only in the $\hat{\mathbf{x}} - \hat{\mathbf{y}}$ plane and $\hat{\mathbf{x}} - \hat{\mathbf{z}}$ plane, respectively. Highlighted contours are $a : \beta = 0.0008$, $b : \beta = 0.008$, $c : \beta = 0.03$, $d : \beta = 0.3$, similarly reproduced as in other literature.[8,16,17,24] The dashed boundaries $S_1(\mathbf{r_1})$ define the shaded areas where the β-contours

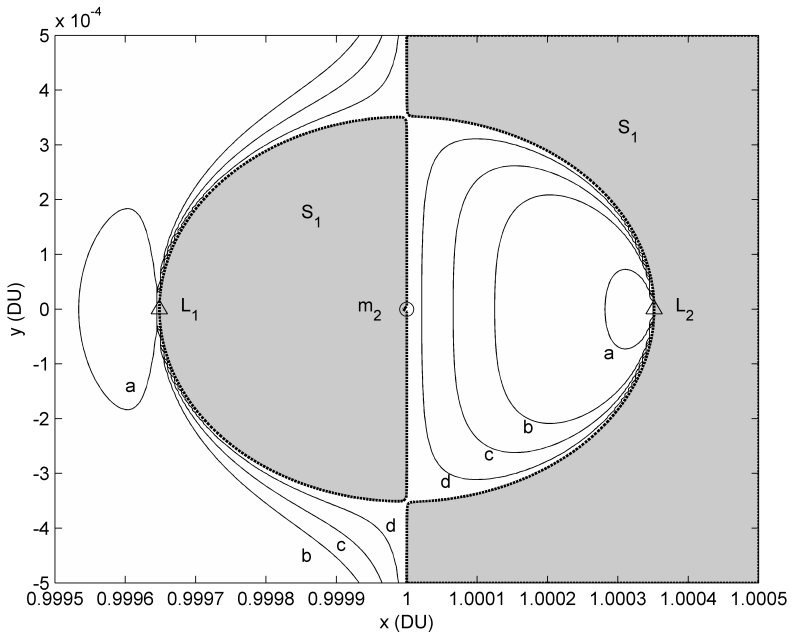

Figure 3. Solar Sail Lightness Number $\beta-$Contours in $\hat{\mathbf{x}} - \hat{\mathbf{y}}$ and $\hat{\mathbf{x}} - \hat{\mathbf{y}}$ Plane

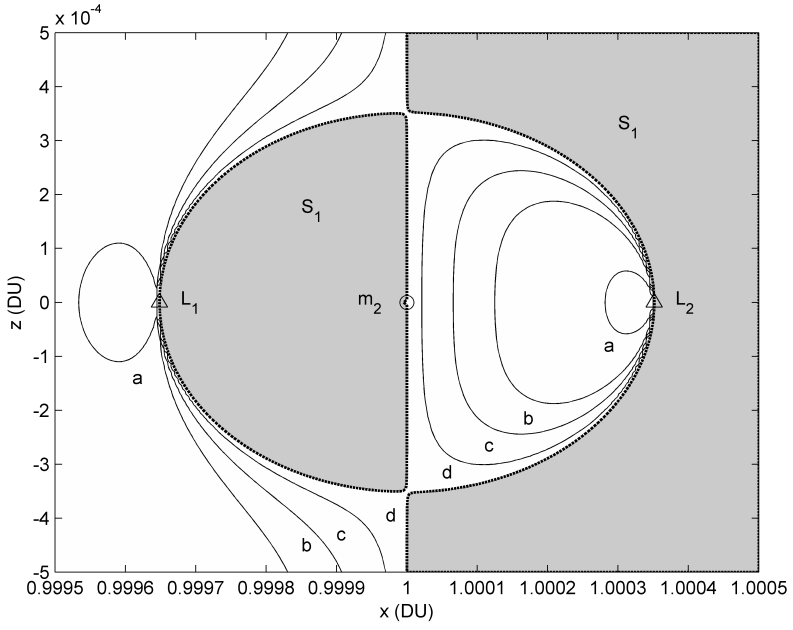

Figure 4. Solar Sail Lightness Number $\beta-$Contours in $\hat{\mathbf{x}} - \hat{\mathbf{z}}$ Plane

cannot exist as $\mathbf{r_1} \cdot \mathbf{n} \geq 0$ and touch the mass m_2 and the collinear points L_1 and L_2, corresponding to the classical solutions with $\boldsymbol{\nabla} U = \mathbf{0}$ or $\alpha = 90^\circ$.

The result clearly complies with the theory, however, since μ is very small then this renders more

flexible solar sail surfing for small numbers of β than for large β, demonstrated to be on the order of 10 less than the Sun-Earth system.[8] What this practically means is that the solar radiation pressure force is smaller than the solar gravitational force or for a balance between the solar radiation pressure force and the solar gravitational force, the area to mass ratio is smaller meaning a smaller solar sail is required for a specific mass. When $0.03 \leq \beta \leq 1$, the contours do not change considerably and thus sail surfing is restricted. If $0 \leq \beta \leq 1$ then the contour shows a 3D nested torus projected onto the $\hat{\mathbf{x}} - \hat{\mathbf{y}}$ or $\hat{\mathbf{x}} - \hat{\mathbf{z}}$ plane. However for $\beta > 1$, then the inner radius of the torus disappears. As $\beta \to \infty$, the libration surfaces approach the boundary $S_1(\mathbf{r_1})$.

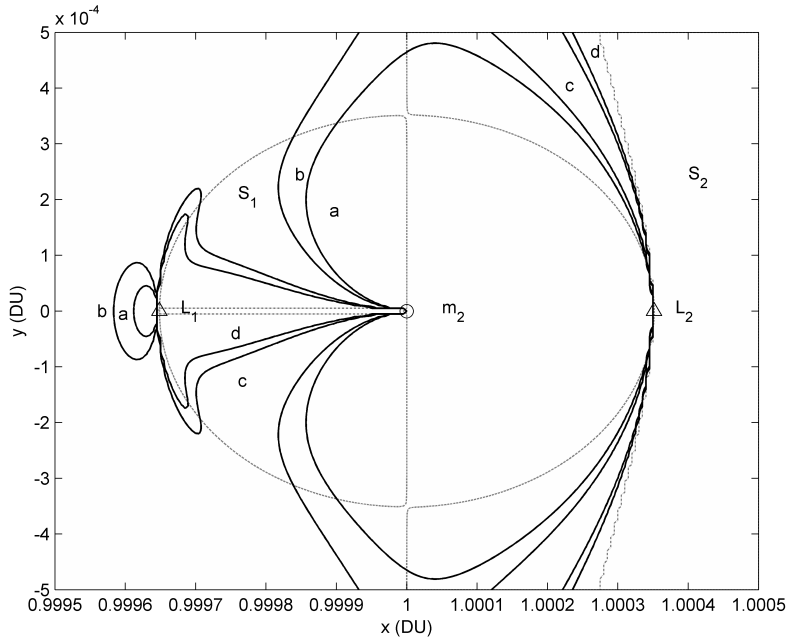

Figure 5. Solar Sail Lightness Number $\beta-$Contours in $\hat{\mathbf{x}} - \hat{\mathbf{y}}$ Plane with Albedo

Figure 5 and 6 shows some of the equilibrium solutions or contours of solar sail lightness number β in the CR3BP with SRP and albedo effects in the $\hat{\mathbf{x}} - \hat{\mathbf{y}}$ plane and $\hat{\mathbf{x}} - \hat{\mathbf{z}}$ plane, respectively. Highlighted contours are $a : \beta = 0.0003$, $b : \beta = 0.0005$, $c : \beta = 0.005$, $d : \beta = 0.01$. The dashed boundaries $S_1(\mathbf{r_1})$ define the shaded areas where the β-contours could not exist for the CR3BP model with SRP only as $\mathbf{r_1} \cdot \mathbf{n} \geq 0$. $S_1(\mathbf{r_1})$ define the shaded areas due to the constraint $\mathbf{r_2} \cdot \mathbf{n} \geq 0$. This new boundary is obviously the important to investigate in future work. The mass m_2 and the collinear points L_1 and L_2, corresponding to the classical solutions with $\boldsymbol{\nabla} U = \mathbf{0}$ or $\alpha = 90^\circ$ and $\psi = 0^\circ$ lie on both of the boundaries.

These results differ from Figure 3 and 4, showing that $\beta-$contours in general have different shape due to the Lambertian BRDF effects. Noteworthy is that closer Sun-side equilibrium points exist between L_1 and m_2 which shows that the albedo from the asteroid could potentially induce beneficial effects on the solar sail. For flexible solar sail surfing then β has to be even smaller than shown in Figure 1 and 2. This time it means the solar sail can move easily with smaller SRP force as it would at some points balance out the gravity and reflected radiation from the asteroid, rendering existence of new equilibrium solutions. When $0.005 \leq \beta \leq \infty$, the contours do not change considerably and surfing is restricted. As $\beta \to \infty$, the libration points approach the boundaries $S_1(\mathbf{r_1})$ and $S_2(\mathbf{r_1})$.

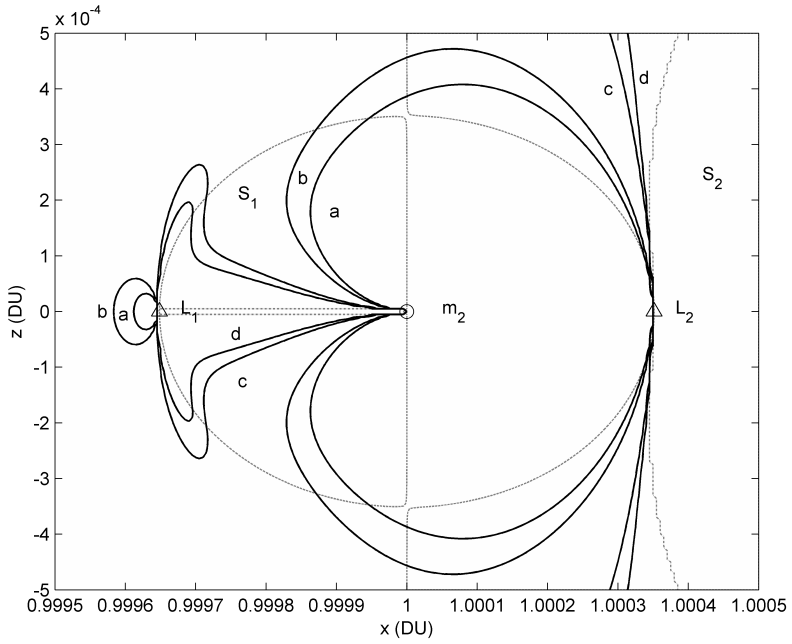

Figure 6. Solar Sail Lightness Number $\beta-$Contours in $\hat{\mathbf{x}} - \hat{\mathbf{z}}$ Plane with Albedo

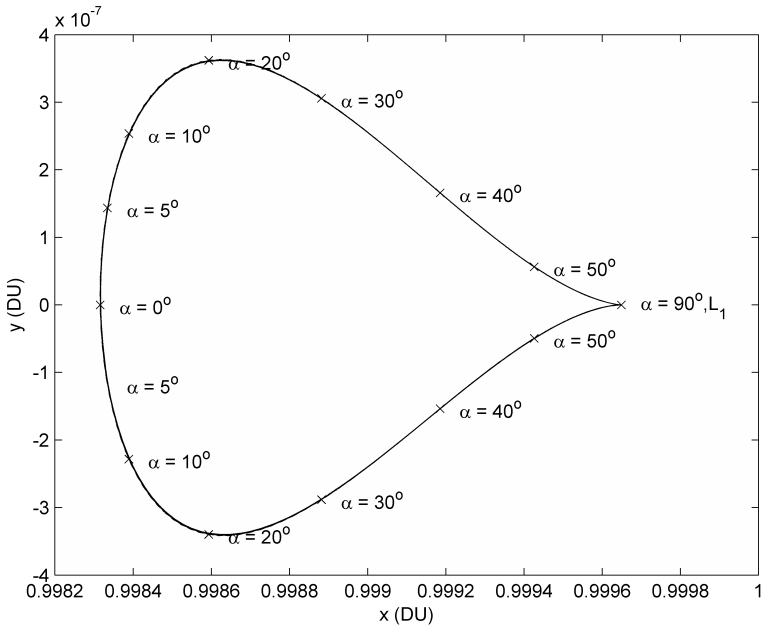

Figure 7. Solar Sail Equilibrium Points for $\beta = 0.005$ with Albedo in $\hat{\mathbf{x}} - \hat{\mathbf{y}}$ Plane

Since F, thus the albedo effect, is a function of the distance r_2, it would be interesting to see how this would affect the equilibrium points outside of the region around L_1 and L_2.

Figure 7 shows a section with the equilibrium points for a constant $\beta = 0.005$ with varying $0^\circ \leq \alpha \leq 90^\circ$ for $\gamma = \pm 90^\circ$ for albedo $\rho = 0.2$. The lower half of the plot corresponds to $\gamma = +90^\circ$ while $\gamma = -90^\circ$. It can easily be seen that at $\alpha = 90^\circ$, the equilibrium point exists at L_1.

CONCLUSIONS & FUTURE WORK

It is clear that adding albedo radiation pressure has significant effects on solar sail dynamics with SRP in CR3BP. The equilibrium points are considerably altered when including the albedo effects in the SRP model for the Sun-Asteroid system. Artificial equilibrium points are found be existing on the Sun-side of the asteroid, which motivates new mission possibilities around these interesting points.

Stability and controllability at libration points, through analyzing local linear dynamics, has been checked and it is found that the equilibrium points are still unstable with albedo effects due to the additional perturbations. Since the libration points are controllable, the solar sail can induce attitude changes as such to enforce asymptotic stability or Lyapunov stability at the points of interest.

For an asteroid or a comet with high albedo it is also important to investigate other dominant effects around primitive bodies as opposed to those conventially expected for terrestrial planets. These findings would be benificial for any type of spacecraft mission to distant planets, asteroids or comets. From an astrodynamics perspective this work would provide a new way to look at long-term missions to bright objects as the albedo effect is especially important to consider for the sensitive surfaces of a solar sail. As an extension to this work, future work will involve analysis of periodic orbits around the artificial on-axis and off-axis equilibrium points, transfers between equilibrium points, oblateness effects, elliptical models for both the Sun-Asteroid and Earth-Asteroid system.

REFERENCES

[1] M.J. Sonter. The technical and economic feasibility of mining the near-earth asteroids. *Acta Astronautica*, 41:637–647, 1997.

[2] D. Nevsvorny et al. Recent origin of the solar system dust bands. *The Astrophysical Journal*, 591(1):486–497, 2003.

[3] D.J. Scheeres et al. The effect of yorp on itokawa. *Icarus*, 188:425–429, 2007.

[4] P. Michel and Makoto Yoshikawa. Earth impact probability of the asteroid (25143) itokawa to be sampled by the spacecraft hayabusa. *Icarus*, 179:291–296, 2005.

[5] C.T. Russell et al. Dawn mission to vesta and ceres. *Earth Moon Planet*, 101:65–91, 2007.

[6] R.W. Farquhar and A.A. Kamel. Quasi-periodic orbits about the translunar libration point. *Celestial Mechanics*, 7:458–473, 1973.

[7] K.C. Howell. Three-dimensional, periodic, 'halo' orbits. *Celestial Mechanics*, 32:53–71, 1984.

[8] A.J.C McDonald C.R. McInnes and J.F.L. Simmons. Solar sail parking in restricted three-body systems. *Journal of Guidance, Control, and Dynamics*, 1994.

[9] A. Farres and A. Jorba. Station keeping of a solar sail around a halo orbit. *Acta Astronautica*, 94:527–539, 2012.

[10] P.L. Lamy J.A. Burns and S. Soter. Radiation forces on small particles in the solar system. *Icarus*, 40:1–48, 1979.

[11] S. V. Ershkov. The yarkovsky effect in generalized photogravitational 3-body problem. *Planetary and Space Science*, 73:221–223, 2012.

[12] D. J. Scheeres and F. Marzari. Spacecraft dynamics in the vicinity of a comet. *Journal of the Astronautical Sciences*, 50(1):35–52, 2002.

[13] S.B. Broschart and D.J. Scheeres. Control of hovering spacecraft near small bodies: Application to asteroid 25143 itokawa. *Journal of Guidance, Control, and Dynamics*, 28:343–354, 2005.

[14] D.J. Scheeres E. Morrow and D. Lubin. Solar sail orbit operations at asteroids. *Journal of Spacecraft and Rockets*, 38:279–286, 2001.

[15] M. Macdonald and C. McInnes. Solar sail science mission applications and advancement. *Advances in Space Research*, 48:1702–1716, 2011.

[16] C.R. McInnes. *Solar Sailing: Technology, Dynamics and Mission Applications*. Springer Praxis, 1999.

[17] A.I.S McInnes. Strategies for solar sail mission design in the circular restricted three-body problem. Master's thesis, Purdue University, 2000.

[18] J.R. Shell. Optimizing orbital debris monitoring with optical telescopes. Technical report, US Air Force, Space Innovation and Development Center, 2010.

[19] P. Magnusson et al. Photometric observations and modeling of asteroids= 1620 geographos. *Icarus*, 123:227–244, 1996.

[20] J. Torppa M. Kaasalainen and J. Piironen. Models of twenty asteroids from photometric data. *Icarus*, 159:369–395, 2002.

[21] D.C. Jewitt Y.R. Fernandez and S.S. Sheppard. Albedos of asteroids in comet-like orbits. *The Astronomical Journal*, 130:308–318, 2005.

[22] M.W. Busch et al. Physical properties of a near-earth asteroid (33342) 1998 wt24. *Icarus*, 195:614–621, 2008.

[23] D.S. Bernstein. *Matrix Mathematics: Theory, Facts and Formulas*. Princeton University Press, 2nd edition, 2009.

[24] J.S. Nuss. The use of solar sail in the circular restricted problem of three bodies. Master's thesis, Purdue University, 1998.